

Gamma-rays from the Large Scale Structure of the Universe

Francesco Miniati

Max-Planck-Institut für Astrophysik, Karl-Schwarzschild-Str. 1, 85740, Garching, Germany

Gamma-ray astronomy will play a crucial role in the investigation of nonthermal processes in the large scale structure of the universe. Particularly, galaxy clusters (GC) observations at this photon energy will help us understand the the origin of radio emitting high energy particles, the possible level of cosmic-ray (CR) pressure in intracluster environment, and the strength of intracluster magnetic fields. In addition here we point out the importance of these observations for a possible detection of cosmic shocks through γ -ray emission and for constraining their CR acceleration efficiency. We model spatial and spectral properties of nonthermal γ -ray emission due to shock accelerated CRs in GC and *emphasize* the importance of imaging capability of upcoming γ -ray facilities for a correct interpretation of any observational results.

1 Introduction

Cosmic shocks emerge during structure formation in the universe, as gravitationally driven gas infall onto collapsing objects becomes supersonic. The dissipation of kinetic energy at these shocks raises the temperature of the intergalactic gas. In galaxy clusters (GC), characterized by accretion velocities of order $\sim 10^3$ km s $^{-1}$, the gas temperature reaches $\sim 10^8$ K. Also, according to recent numerical simulations most of the low redshift baryons, observed at high redshift as Ly- α absorbers have been shock heated to a temperature of $10^5 - 10^7$ K 1 .

Astrophysical shocks are collisionless and it is believed that as part of the dissipation mechanism supra-thermal populations of particles (cosmic-rays, CR hereafter) are generated via first order Fermi mechanism 2 . Both CR protons and electrons can be accelerated. CR electrons are characterized by rather short radiative lifetime. For a typical intra-cluster environment, the main loss mechanism is inverse Compton (IC) for energies above ~ 150 MeV and Coulomb losses below that. Low energy, sub-relativistic CR protons also suffer Coulomb losses as electrons of the same energy. However, for relativistic protons the dominant energy loss mechanism up to the energy threshold for photo-pair production is p-p inelastic collisions with a timescale longer than a Hubble time. Therefore, once accelerated CR protons up to $\sim 10^{15}$ eV accumulate within large scale structures where they can be confined by μ G strong turbulent magnetic fields 3 .

It is of interest to investigate the acceleration of CRs at cosmic shocks for a number of reasons. Firstly, GCs exhibit non-thermal radiation. This mainly consists of diffuse radio emission extending on Mpc scales. It is thought to be synchrotron radiation but there is no consensus as to the origin of the emitting relativistic electrons. In addition, excess of radiation with respect to thermal emission has been reported at both hard X-ray 4 and, although more controversially, for the extreme ultraviolet part of the spectrum 5,6 . Secondly, if shocks acceleration operates efficiently, the proton component could bear a significant fraction of the total gas pressure, affecting the dynamics of cosmic structures 7 . Finally, CR electrons accelerated at inter-galactic shocks could contribute a significant fraction of the cosmic γ -ray background (CGB) 8 .

In this contribution we address the role of γ -ray observations for investigating CR acceleration at large scale structure shocks. The results presented here are based on a numerical simulation which is briefly described in §2. In §3 we address the contribution of cosmological CRs to the CGB and, based on EGRET experimental results, we constraint the efficiency of shock acceleration of CR electrons. In §4 we present the non-thermal spectrum at γ -ray energies for a Coma cluster prototype and in §5 we discuss the importance of γ -ray observations for investigating physical conditions in intra-cluster medium (ICM) environment.

2 Numerical set-up

We perform numerical simulations that model simultaneously the formation of the large scale structure and the acceleration, transport and energy losses of three CR species: namely *shock accelerated* (primary) protons and electrons and secondary e^\pm generated in p-p inelastic collisions of the simulated CR protons and the thermal nuclei of the IGM. The simulation is fully described elsewhere⁹ and here we shall only summarize the most important aspects of it.

As for the large scale structure we adopt a canonical, flat Λ CDM model with total mass density $\Omega_m = 0.3$, vacuum energy density $\Omega_\Lambda = 1 - \Omega_m = 0.7$, normalized Hubble constant $h \equiv H_0/100 \text{ km s}^{-1} \text{ Mpc}^{-1} = 0.67$, baryonic mass density, $\Omega_b = 0.04$, and spectral index and cluster normalization for initial density perturbations, $n_s = 1$ and $\sigma_8 = 0.9$ respectively.

The CR dynamics, including injection at shocks, acceleration, energy losses/gains and spatial transport, is computed numerically through the code COSMOCR^{10,9}. CR protons are injected at shocks according to thermal leakage prescription. With the adopted parameters, a fraction about 10^{-4} of the particles crossing the shock is injected as CRs. For shocks with Mach number between 4 and 10, which are responsible for most of the heating of the IGM⁹, this roughly corresponds to converting 30% of the shock ram pressure into CR proton pressure. The injection of primary CR electrons in the acceleration mechanism is here simply modeled by assuming that their number ratio to protons at relativistic energies be given by a parameter $R_{e/p}$. Observations^{11,12} typically indicate $R_{e/p} \sim 10^{-2}$. In accord to the test particle limit of diffusive shock acceleration theory², the injected particles are redistributed in momentum as a power-law with slope related to the shock Mach number, M , as: $q = 4/(1 - M^{-2})$. Each CR population is passively advected with the flow. Finally, energy losses/gains of the accelerated CRs are followed by solving numerically a “kinetic” equation written in comoving coordinates and integrated over a discrete set of logarithmically equidistant momentum intervals that define the numerical grid in momentum space¹⁰. We follow CR protons in the momentum range between 0.1 GeV/c and 10^6 GeV/c, and CR electrons and e^\pm between 15 MeV/c and 20 TeV/c.

3 Contribution to the Cosmic Gamma-ray Background

In Fig. 1⁹ (left) we illustrate the contribution to the CGB from CRs accelerated at cosmic shocks, together with observational data taken from the EGRET experiment¹³(solid dots). The plot shows as a function of photon energy, ε , the quantity

$$\varepsilon^2 J(\varepsilon) = \varepsilon \frac{c}{4\pi H_0} \int_0^{z_{max}} \frac{e^{-\tau_{\gamma\gamma}}}{[\Omega_m(1+z)^3 + \Omega_\Lambda]^{1/2}} \frac{j[\varepsilon(1+z), z]}{(1+z)^4} dz \quad (1)$$

where $j(\varepsilon, z)$ is the computational-box-averaged spectral emissivity in units ‘photons $\text{cm}^{-3} \text{s}^{-1}$ ’, computed at each simulation red-shift, z , and at the appropriately blue-shifted photon energy $\varepsilon(1+z)$. In addition, $\tau_{\gamma\gamma}$ is an attenuation factor due to photo-pair creation, $\gamma\gamma \rightarrow e^\pm$, c indicates the speed of light and z_{max} an upper limit of integration. We consider the following emission processes: IC emission of CR electrons scattering off cosmic microwave background photons (dot line), decay of neutral pions ($\pi^0 \rightarrow \gamma\gamma$) produced in p-p inelastic collisions (dash

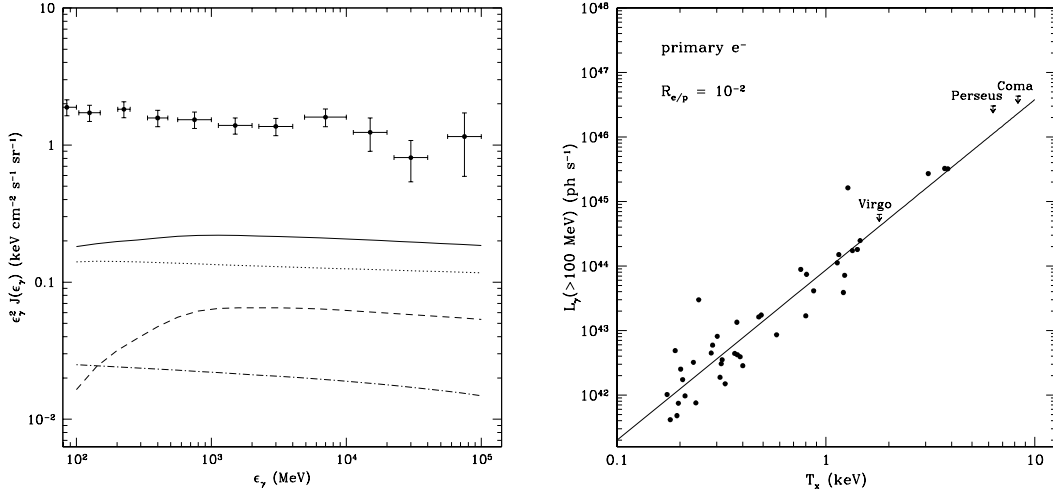


Figure 1: *Left*: Total γ -ray background flux produced by cosmological CRs (solid line), contributions from IC emission from primary CR electrons (dot line), π^0 -decay (dash line) and IC from secondary e^\pm (dash-dot line), and EGRET experimental data with their error-bars (solid dots)¹³ *Right*: The IC γ -ray photon luminosity above 100 MeV from individual clusters as a function of the cluster X-ray core temperature, T_x . The flux is produced by CR electrons accelerated at accretion shocks onto GC. EGRET experimental upper limits are from Reimer¹⁴.

line) and IC emission from secondary e^\pm (dot-dash line). In fig. 1 the total flux (solid line) corresponds roughly to a constant value at the level of $0.2 \text{ keV cm}^{-2} \text{ s}^{-1} \text{ sr}^{-1}$ throughout the spectrum. It is dominated by IC emission from primary electrons. A fraction of order 30% and 10 % is produced by π^0 -decay and IC emission from secondary e^\pm respectively.

Remarkably, all three components produce the same flat spectrum, similar in shape to the observed one. This result is a reflection of the fact that the CRs distributions producing the γ -ray radiation were generated in strong shocks with a log-slope $q \simeq 4^9$. However, the computed flux is only $\sim 15 \%$ of the observed CGB. It is difficult to imagine a higher contribution from π^0 -decay (dash line) and IC emission from e^\pm (dot dash line). In fact, if more CR protons were produced at shocks, CR-induced shock modifications would actually end up reducing the population of γ -ray emitting protons (and e^\pm). It is possible, however, at least in principle that CR electrons would be accelerated more efficiently than assumed here. In fact, by setting $R_{e/p} = 10^{-2}$ we assume that for strong shocks a fraction $\eta \sim 4 \times 10^{-3} [\log(p_{max}/m_e c) / \log(4 \times 10^7)]$ (p_{max} is the maximum momentum of the accelerated electrons) of the shock ram pressure is converted into CR electrons. This is an important matter because if one assumes that η is of order of a few percent then the origin of the unexplained component of the CGB could be accounted for⁸.

However, the electron acceleration efficiency can be constrained by comparing the simulated clusters' γ -ray photon luminosity above 100 MeV to the upper limits set by the EGRET experiment^{15,14} for nearby GCs. This is done in fig. 1⁹ (right panel). The best-fit to the plotted data (solid curve) was found through a least- χ^2 analysis to be:

$$L_\gamma(> 100 \text{ MeV}) = 8.7 \times 10^{43} \left(\frac{\eta}{4 \times 10^{-3}} \right) \left(\frac{T_x}{\text{keV}} \right)^{2.6} \text{ ph s}^{-1}. \quad (2)$$

According to our calculations, the EGRET upper limits (particularly those relative to Coma and Virgo clusters) require that $\eta \leq 0.8\%$. For the adopted proton injection efficiency this roughly translates into $R_{e/p} \leq 2 \times 10^{-2}$. In any case, this implies an upper limit on the computed γ -ray flux of about $0.35 \text{ keV cm}^{-2} \text{ s}^{-1} \text{ sr}^{-1}$. Thus, according to our computation, cosmological CRs could contribute an important fraction of order $\sim 25 \%$ of the CGB.

4 γ -ray for a Coma-cluster prototype: synthetic emission maps and spectrum

In this section we explore the spectral and spatial properties of non-thermal γ -ray radiation between 10 keV and 10 TeV due to shock accelerated CRs in GC. Clusters observations in this photon energy range are important for a number of issues which we address in detail in the discussion section. Among these are the following: correct measurements of intra-cluster magnetic field, estimate of CR proton pressure component, possible detection of cosmic shocks, estimate of CR acceleration efficiency. However, for a correct interpretation of the observational results it is important that the emission produced by different particle components be properly identified. In this respect, the results presented in the following are aimed at helping a correct diagnostic of future γ -ray observations.

As non-thermal bremsstrahlung turns out unimportant¹⁶, we consider the following emission processes: π^0 -decay and IC emission from both primary CR electrons and secondary e^\pm . We first compute the emission spectrum for the largest virialized object in the computational box which has an X-ray core temperature $T_x \simeq 4$ keV. The various emission components are then renormalized to the case of a Coma-like cluster. In particular, IC emission from electrons is rescaled according to equation 2. The total number of e^\pm is rescaled assuming that these particles are responsible for the synchrotron emission of Coma radio halo. For the purpose we took a radio flux at 1.4 GHz $S_{1.4GHz} = 640$ mJy¹⁷ and a volume average magnetic field $\langle B \rangle \sim 3\mu\text{G}$.¹⁸ For the ensuing discussion it is not necessary to assume that the CRs responsible for the synchrotron emission are secondary e^\pm . We know that these high energy particles exist from the observed radio flux and the morphology of radio halos suggest that they reside in the inner region of clusters. However, assuming that these are secondary e^\pm allows us to also normalize the rate of p-p inelastic collisions that determine the total π^0 -decay flux.

The simulation results indicate that the radiation emitted by primary CR electrons and both π^0 -decay as well as secondary e^\pm originates in spatially separate regions. This is a reflection of both the spatial distribution of the emitting particles as well as the nature of the emission process. Thus, on the one hand, both e^\pm and π^0 are produced at the highest rate in the densest regions where both the parent CR ions and target ICM nuclei are most numerous. Consequently, IC from e^\pm and π^0 -decay emissivities are strongest in the cluster inner regions and quickly fade toward its outskirts. On the other hand, because of severe energy losses, γ -ray emitting high energy primary electrons are only found in the vicinity of strong shocks where they are being accelerated. Thus, because the strongest shocks are located at the cluster outskirts rather than at its core where the ICM temperature is high¹⁹, the spatial distribution of the emissivity is now reversed with respect to the previous case. In the four left panels of fig. 2 we present synthetic maps of the integrated photon flux above 100 keV (top panels) and 100 MeV (bottom panels). Among these four panels, the right panels are associated with IC emission from primary electrons and the left panels to IC from secondary e^\pm (top-left) and π^0 -decay (bottom-left). As anticipated the emission from π^0 -decay (bottom left) and e^\pm (top left) is confined to the cluster core. There it creates a diffuse halo which rapidly fades with distance from the center. On the other hand, IC emission from primary e^- is distributed over a much more extended area. Moreover, it is characterized by a strikingly rich and irregular structure. This is a direct reflection of the complex “web” of shocks that reside at the outskirts of galaxy clusters¹⁹.

After generating multifrequency synthetic maps that include all the aforementioned emission components, in the central panel of fig. 2 we have produced synthetic spectra extracted from a core (top) and an outskirts region (bottom). The core region corresponds to an angular size of 1° and the outskirts region is defined as a ring with inner and outer radii of 0.5° and 1.5° respectively ($0.5^\circ \sim 1$ Mpc at the red-shift of Coma cluster). Based on the above findings, the idea is that by looking at the cluster core one should see the π^0 -decay and e^\pm contributions whereas by observing the outskirts one should see IC emission from CR electrons accelerated at

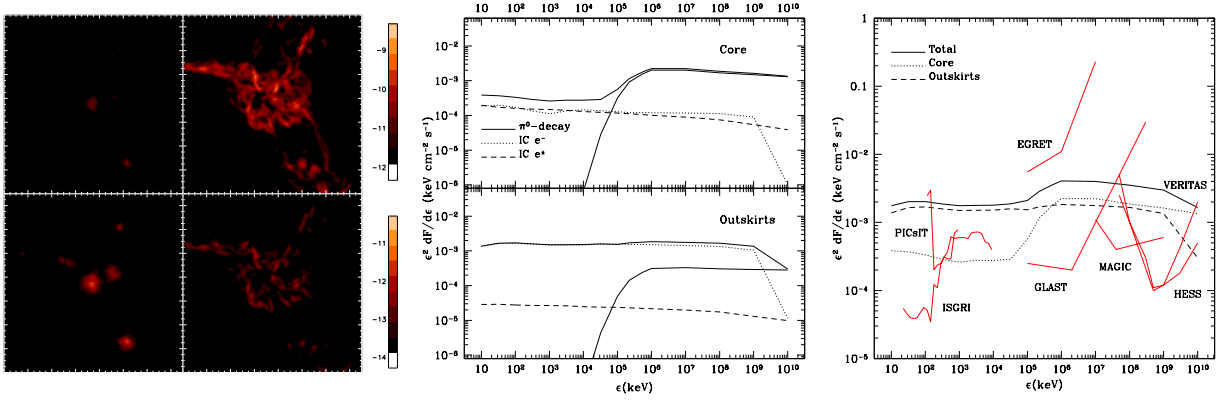


Figure 2: *Left:* Synthetic map of the integrated photon flux above 100 keV (top) and 100 MeV (bottom) in units “ $\text{ph cm}^{-2} \text{s}^{-1} \text{arcmin}^{-2}$ ” from IC emission by secondary e^\pm (top-left), primary e^- (top-right, bottom-right), and π^0 -decay (bottom-left). Each panel measures $15 h^{-1}\text{Mpc}$ on a side. *Center:* Synthetic spectra from 10 keV up to 10 TeV extracted from a core (top) and an outskirts region (bottom). *Right:* Comparison of synthetic spectra with nominal sensitivity limits of future γ -ray observatories (thick-solid lines). For INTEGRAL-IBIS imagers (ISGRI and PICsIT) the curves correspond to a detection significance of 3σ with an observing time of 10^6 s. All other sensitivity plots refer to a 5σ significance. EGRET and GLAST sensitivities are shown for one year of all sky survey and Cherenkov telescopes (MAGIC, VERITAS and HESS) for 50 hour exposure on a single source.

accretion shocks. Fig. 2 (center) shows that at high photon energy (> 100 MeV) the spectrum of radiation is indeed dominated by π^0 -decay (solid thin line) in the core region (top panel) and by IC emission (dotted line) from primary electrons in the outer region (bottom). Below ~ 100 MeV the flux from the outskirts region is still strongly dominated by IC emission from primary e^- . This contribution is much reduced in the narrower field of view of the core region. However it is still significant and at the level of IC emission from secondary e^\pm . Because the radiation flux from these two components depends on the assumed normalizations and the actual shock structure subtended by the field of view, their almost equality in fig. 2 (center, top panel) is obviously only indicative. Nevertheless they are expected of comparable intensity. The contribution of the primary CR electrons could be estimated by measuring its radial dependence in the outer regions, where it dominates, and then by extrapolating its value for the core region.

5 Discussion

In the right panel of fig. 2 we plot sensitivity limits of planned γ -ray observatories together with the total radiation spectra from the core (dotted line) and outskirts (dashed line) regions. The sensitivity limits are plotted for point sources and will be somewhat worse for the case of clusters given their large angular size. In any case, according to this plot, several future experiments should be sensitive enough to detect the computed non-thermal emission at most photon energies. In particular the IBIS imager onboard INTEGRAL should readily measure the flux between 100 keV and several MeV. In addition GLAST and Cherenkov telescopes should be able to detect both the core γ -ray emission from π^0 -decay as well as the IC flux directly produced at accretion shocks above 100 MeV and 10 GeV respectively.

These measurement will provide important information about GCs. First, the extended emission is produced at the location of accretion shocks. Merger shocks have occasionally been observed in the core of clusters as relatively weak temperature jumps. However, strong accretion shocks have yet to be observed *directly*. Thus, detection and imaging of IC emission from primary electrons would provide an opportunity to directly observe GC accretion shocks.

Furthermore, measuring the flux about 100 keV together with radio measurements, will

allow an estimate of (or upper limits on) the ICM magnetic field. It is important, however, to separate out the contribution from the CR electrons accelerated at the outlining shocks. Because the magnetic field strength is expected to drop at the cluster outskirts, these electrons likely generate only a weak radio emission. Nonetheless, they produce a strong IC flux which can easily dominate the total soft γ -ray emission (cf. fig. 2). In this case separating out their contribution would be an important step for correctly measuring ICM magnetic fields.

One of the most awaited experiments is related to the measurement of the γ -ray flux at and above 100 MeV. This is important in order to convalidate or rule out secondary e^\pm models for radio halos in GC^{20,21,22} and in order to estimate the non-thermal CR pressure there⁷. In this perspective several authors estimated for nearby clusters the γ -ray flux from π^0 -decay. However, radiation flux from IC emission can be comparable¹⁶. Therefore, for a correct interpretation of the measurements the contributions from these two components will need to be separated as outlined here. Estimating the γ -ray flux from IC emission due to primary CR electrons will also be instrumental for addressing the contribution of this emission mechanism to the CGB^{8,9,23}.

Measurements at photon energies, from $\sim 10 - 100$ GeV to $1 - 10$ TeV, will also be of great interest. Because the radiated energy spectrum is directly connected to the distribution function of the emitting particles, measuring the flux at different energies will provide information about the acceleration mechanism. In particular, the observed spectrum could differ from our predictions if the accretion shocks were modified by CR pressure. Finally the maximum energy of the accelerated CR electrons could be inferred from a spectral cut-off, although only as long as the latter turns out below the energy threshold for $\gamma\gamma$ absorption (\sim TeV). Given the different environmental conditions with respect to supernova remnants, observations of galaxy clusters offer the interesting possibility for a broad exploration of shock acceleration physics.

Bibliography

1. Cen, R. & Ostriker, J. P. 1999, *ApJ*, 514, 1
2. Blandford, R. D. & Eichler, D. 1987, *Phys. Rep.* , 154, 1
3. Völk, H. J., Aharonian, F. A., & Breitschwerdt, D. 1996, *Space Sci. Rev.* , 75, 279
4. Fusco-Femiano, R., et al. 1999, *ApJ*, 513, L21
5. Lieu, R., et al. 1996, *Science* , 274, 1335
6. Bowyer, S., Berghoefer, T. W., & Korpela, E. 1999, *ApJ*, 526, 592
7. Miniati, F., Ryu, D., Kang, H., & Jones, T. W. 2001, *ApJ*, 559,
8. Loeb, A. & Waxman, E. 2000, *Nature (London)* , 405, 156
9. Miniati, F. 2002, *MNRAS*, submitted (astro-ph/0203014)
10. Miniati, F. 2001, *Comp. Phys. Comm.* , 141, 17
11. Müller, D. & et al. 1995, in *Int. Cosmic Ray Conference*, Vol. 3, Rome, 13
12. Allen, G. E., Petre, R., & Gotthelf, E. V. 2001, *ApJ*, 558, 739
13. Sreekumar, et al. 1998, *ApJ*, 494, 523
14. Reimer, O. 1999, in *ICRC*, Vol. 4, ed. D. Kieda, et al., Salt Lake City, Utah, 89
15. Sreekumar, et al. 1996, *ApJ*, 464, 628
16. Miniati, F. 2002, *MNRAS*, submitted
17. Deiss, B. M., Reich, W., Lesch, H., & Wielebinski, R. 1997, *A&A*, 321, 55
18. Kim, K.-T., Kronberg, P. P., Dewdney, P. E., & Landecker, T. L. 1990, *ApJ*, 355, 29
19. Miniati, F., Ryu, D., Kang, H., Jones, T. W., Cen, R., & Ostriker, J. 2000, *ApJ*, 542, 608
20. Dolag, K. & Enßlin, T. 2000, *A&A*, 362, 151
21. Blasi, P. & Colafrancesco, S. 1999, *Astropart. Phys.* , 12, 169
22. Miniati, F., Jones, T. W., Kang, H., & Ryu, D. 2001, *ApJ*, 562, 233
23. Keshet, U., et al. 2002, *ApJ*, (astro-ph/0202318)